



Research Article

Platelet-rich plasma accelerates skin wound healing by promoting re-epithelialization

Pengcheng Xu^{1,#}, Yaguang Wu^{2,#}, Lina Zhou³, Zengjun Yang², Xiaorong Zhang^{4,5}, Xiaohong Hu^{4,5}, Jiakai Yang^{4,5}, Mingying Wang^{4,5}, Binjie Wang^{4,5}, Gaoxing Luo^{4,5,*}, Weifeng He^{4,5,*}, and Biao Cheng^{1,*}

¹Department of Burn and Plastic Surgery, General Hospital of Southern Theater Command, PLA, Guangzhou, China, ²Department of Dermatology, Southwest Hospital, Third Military Medical University (Army Medical University), Chongqing, China, ³Department of Endocrinology, Southwest Hospital, Third Military Medical University (Army Medical University), Chongqing, China, ⁴State Key Laboratory of Trauma, Burn and Combined Injury, Institute of Burn Research, Southwest Hospital, Third Military Medical University (Army Medical University), Chongqing 400038, China, and ⁵Chongqing Key Laboratory for Disease Proteomics, Chongqing 400038, China

*Correspondence. Gaoxing Luo, Email: logxw@yahoo.com; Weifeng He, Email: whe761211@hotmail.com; Biao Cheng, Email chengbiaocheng@163.com.

Joint first authors.

Received 6 March 2020; Revised 24 April 2020; Editorial decision 11 June 2020

Abstract

Background: Autologous platelet-rich plasma (PRP) has been suggested to be effective for wound healing. However, evidence for its use in patients with acute and chronic wounds remains insufficient. The aims of this study were to comprehensively examine the effectiveness, synergy and possible mechanism of PRP-mediated improvement of acute skin wound repair.

Methods: Full-thickness wounds were made on the back of C57/BL6 mice. PRP or saline solution as a control was administered to the wound area. Wound healing rate, local inflammation, angiogenesis, re-epithelialization and collagen deposition were measured at days 3, 5, 7 and 14 after skin injury. The biological character of epidermal stem cells (ESCs), which reflect the potential for re-epithelialization, was further evaluated *in vitro* and *in vivo*.

Results: PRP strongly improved skin wound healing, which was associated with regulation of local inflammation, enhancement of angiogenesis and re-epithelialization. PRP treatment significantly reduced the production of inflammatory cytokines interleukin-17A and interleukin-1 β . An increase in the local vessel intensity and enhancement of re-epithelialization were also observed in animals with PRP administration and were associated with enhanced secretion of growth factors such as vascular endothelial growth factor and insulin-like growth factor-1. Moreover, PRP treatment ameliorated the survival and activated the migration and proliferation of primary cultured ESCs, and these effects were accompanied by the differentiation of ESCs into adult cells following the changes of CD49f and keratin 10 and keratin 14.

Conclusion: PRP improved skin wound healing by modulating inflammation and increasing angiogenesis and re-epithelialization. However, the underlying regulatory mechanism needs to be

investigated in the future. Our data provide a preliminary theoretical foundation for the clinical administration of PRP in wound healing and skin regeneration.

Key words: Wound healing, platelet-rich plasma, Inflammation, Re-epithelialization, Angiogenesis, Collagen deposition, Epidermal stem cells

Background

Platelet-rich plasma (PRP) is an autologous blood-derived product that contains a high concentration of platelets in plasma. It is derived from whole blood by centrifugation. Activated platelets in PRP can release multiple growth factors and cytokines, including platelet-derived growth factor (PDGF), basic fibroblast growth factor (bFGF), vascular endothelial growth factor (VEGF), insulin-like growth factor-1 (IGF-1) and transforming growth factor- β (TGF- β), and others that are involved in promoting tissue repair and regeneration [1]. Because of its simple preparation, high growth factor content and low immunogenicity, PRP has been widely used in various surgical operations and clinical treatments and has shown promising experimental and clinical effects in wound healing, especially in chronic wounds [2–4].

The essential role of PRP in tissue regeneration and wound healing has been confirmed by many studies. Some researchers' findings suggest that PRP has a strong effect on vascularization. PRP can release a higher content of VEGF to promote the vascularization of deep partial-thickness burns, which is beneficial to the prognosis of burn wounds [5].

PRP can provide an appropriate microenvironment for bone marrow stromal cells (BMSCs) and cooperate with BMSCs to promote diabetic wound healing by promoting angiogenesis and cell proliferation, and by inducing TGF- β 1 expression [6]. Additionally, PRP can promote the formation of new capillaries in a transplanted skin flap and accelerate the local revascularization of the wound [7, 8].

In addition, it has been reported that PRP can release a series of antibacterial substances, reduce local inflammation and prevent wound infection [9]. However, compared with the study of vascularization, the theoretical evidence for these effects is relatively weak.

In addition, PRP is used in the clinical treatment of acute and chronic wounds in an unconventional manner with good results. PRP can increase the healing rate of diabetic wounds, reduce the injury area of pressure ulcers and improve joint function in osteoarthritis (OA) [10–12].

Nevertheless, although the clinical effects of PRP are remarkable and the corresponding basic research has partially revealed the role of PRP from some perspectives, it is still not comprehensive and there is a lack of systematic exposition to evaluate the effects of PRP at different stages of wound healing.

In this study, we made a full-thickness wound model in mice and locally injected mouse-derived PRP to systematically observe the regulatory effects of PRP at different stages of wound healing and the biological functions of epidermal cells. The aim was to provide a certain basis and reference value for

identifying the mechanisms of wound healing promotion and to apply these results rationally in the clinic.

Methods

Experimental animals and model for wound healing

Forty clean-grade male C57/BL6 mice, aged from 6 to 8 weeks, weighing ~25–30 g, were provided by the Experimental Animal Center of the Third Military Medical University (Army Medical University), raised by the Animal Center of Southwest Hospital of Chongqing. The mice were kept under controlled conditions, including a constant temperature of ~18–25°C and a constant humidity of ~50%, allowing them free access to ordinary food and filtered water, and alternating light and darkness for 12 h a day. Five mice were kept per cage before the wound model was prepared, and after making the model the mice were kept one to a cage.

The entire experimental process complies with the ethical standards of experimental animals, and the laboratory personnel have the qualifications of Chongqing animal experiment practitioners. Forty mice were randomly divided into two groups, including a saline control group and a PRP group, and both were evaluated at days 3, 5, 7 and 14.

Mice were anesthetized with 1% pentobarbital sodium solution (0.006 mL/g), their skin was shaved, and the surgeries were performed under standard sterile conditions. Two circular, full-thickness 6 mm diameter cutaneous wounds were created on the back of each mouse. Immediately after the skin injuries, each wound was injected with 100 μ L of PRP activated by the repeated freeze–thaw method. Control wounds were injected with saline solution.

PRP preparation

The mice were anesthetized with 1% pentobarbital sodium solution (0.006 mL/g). PRP was obtained through centrifugation of inferior vena cava blood collected from healthy mice into 0.3% heparin sodium anticoagulant tubes. The plasma was first collected by centrifugation (300 \times g, 10 min). Platelets in the plasma were then concentrated through a second centrifugation (300 \times g, 20 min). Approximately 10 mL of whole blood can produce an average of 2–3 mL of PRP, which was activated by the repeated freeze–thaw method.

Primary culture and identification of epidermal stem cells

The skin of newborn mice was obtained by blunt separation and then disinfected by soaking in 75% alcohol and

washed twice with cold phosphate buffer saline (PBS). The subcutaneous tissue was cut off and then the tissue block was soaked overnight in 0.5% neutral protease at 4°C. The separated epidermis was finely chopped and digested with 0.25% trypsin-EDTA (Gibco, USA) at 37°C for 10 min and the digestion was terminated by trypsin inhibitor (Gibco, USA). After centrifugation (1200 rpm/5 min), the supernatant was filtered with a 200-mesh sieve. At a cell density of 2×10^6 cells/25 cm², the cells were inoculated into six-well plates and cultured in a CO₂ incubator at 37°C. The primary cells were identified by biomarker systems CD49f/CD71 and Keratin 10 (K10), Keratin 14 (K14) and Keratin 15 (K15). CD49f or K15 represents epidermal stem cells, K14 represents transit amplifying cells (TAC) and K10 represents postmitotic differentiating cells (PMD).

Wound closure analysis and morphological observation

Photographs were taken on days 0, 3, 5 and 7 after surgery. The image analysis software (ImageJ) was used to measure the closed wound area and W_0 was defined as the initial wound area. We used ImageJ software to carefully draw the reserved wound area (W_t) along the edge of the wound at each observation time point, and then we calculated the drawing area.

The wound healing rate (% of closed wound area) was determined by the following equations:

$$W\% \text{ (Percent of closed wound area)} = (W_0 - W_t) / W_0 \times 100\%$$

W_0 = the initial wound area

W_t = the residual wound area.

Samples were taken on days 3, 5, 7 and 14. The excised patches, which contained the wound and normal tissue within 5 mm from the wound edge, were fixed in 4% paraformaldehyde, embedded in paraffin, sectioned at 5 μm, and stained with hematoxylin and eosin (H&E) and Masson staining for microscopic observation. The wound contraction distance and the length and thickness of the neo-epidermis were measured by ImageJ software. The actual distance between the neo-epidermis was used to judge the re-epithelialization ability and the length of the epithelial tongue. The vertical distance between the margins of the wound was used to judge the wound contraction.

Immunohistochemistry staining

The paraffin sections were dewaxed and rehydrated by xylene and gradient alcohol, and then were subjected to heat-mediated antigen retrieval. Endogenous peroxidase was inactivated by treatment with 3% H₂O₂ for 10 min at room temperature, blocked with 10% normal goat serum (ZSGB-Bio, China) for 30 min at room temperature, and then incubated with primary antibodies overnight at 4°C. Then, the sections were incubated with biotinylated secondary antibodies (ZSGB-Bio, China) at room temperature for 30 min.

All sections were colored by diaminobenzidine solution (ZSGB-Bio, China) and the nuclei were counterstained with hematoxylin (Beyotime, CN, USA). Then, the sections were photographed using a microscope (Olympus, Japan). Positive results were quantified by Image-Pro Plus (IPP) software in a blinded fashion. Three sections were randomly selected from the PRP group and the control group for staining, and then each section was randomly collected with five high-power fields, which are the top, bottom, left, right and middle of the image. The average value of positive cells or optical density was calculated by means of IPP.

The primary antibodies involved are as follows. Inflammation-associated antibodies: interleukin-1β (IL-1β) (1: 50, Abcam, UK), interleukin-23 (IL-23) (1:400, Abcam, UK), tumor necrosis factor-α (TNF-α) (1:300, Abcam, UK) and interleukin-17 (IL-17) (1:500, Abcam, UK). Angiogenesis-related antibodies: platelet endothelial cell adhesion molecule-1 (CD31) (1:100, Abcam, UK), VEGF (1:100, Abcam, UK), α-smooth muscle actin (α-SMA) (1:150, Abcam, UK), proliferating cell nuclear antigen (PCNA) (1:200, Abcam, UK), TUNEL (Abcam, UK) and IGF-1 (1:200, Abcam, UK).

Observation of the biological function of epidermal stem cells

Cell migration Epidermal stem cells (ESCs) were seeded in a 6-well plate at 6×10^2 cells/well and grown to 80% confluence. Cells were starved ~8–12 h before scratching. Mitomycin C (Sigma Aldrich, USA), 10 μg/mL, was added 2 h before scratching to inhibit proliferation. The cells were scratched with a yellow pipette tip (200 μL) and washed twice with PBS. Thereafter, the cells were stimulated with 2.5% PRP in ESC Special Medium without growth factors. Migration images were captured every 24 h for 72 h at 37°C and 5% CO₂ on a microscope with a 4× objective (Olympus, Japan). The scratch distance was measured manually with ImageJ software, and the distance at $t = 0$ h represented the initial distance. The migration rate was calculated based on the remaining distance at each time point.

Cell proliferation Cells were incubated with EdU (5 μM/well, Invitrogen, USA) for more than 24 h according to the manual's recommendations. Then, the experimental group was treated with 2.5% PRP in ESC Special Medium without growth factors, while the control group received no special treatment. After the cells had been cultured for 24 h, they were treated according to the manufacturer's instructions and analyzed with a flow cytometer (Attune, Applied Biosystems AB, USA).

Cell differentiation ESCs were seeded in a 6-well plate at 6×10^2 cells/well and grown to ~50% confluence. The cells in the experimental group were treated with 2.5% PRP in ESC Special Medium without growth factors, and the control

group received no special treatment. After culturing for 48 h, the cells were resuspended in cold PBS and centrifuged at 1700 rpm for 5 min. Then, each group was mixed with 200 μ L PBS and 1 μ L of the specified antibodies, including CD71/CD49f (1:100, Becton, Dickinson and Company, USA) and K10/K14 (1:100, Santa Cruz, USA). After incubation at room temperature away from light for 1 h, each group was washed and resuspended in 600 μ L of PBS and detected by flow cytometry within 1 h. The expression of biomarkers before and after PRP treatment was observed and recorded.

Cell apoptosis The cells were stimulated with 2.5% PRP in ESC Special Medium without growth factors for 6 h, then collected by centrifugation (1700 rpm/5 min). The cells were washed with PBS by pipetting them up and down. The cells were resuspended in 200 μ L of binding buffer (1 \times) to a density of 5×10^5 /mL. Then, we added 5 μ L of Annexin V-FITC to 195 μ L of the cell suspension. It was mixed and incubated for 10 min at room temperature. The cells were washed in 200 μ L binding buffer (1 \times) and resuspended in 190 μ L of binding buffer (1 \times). Then, we added 10 μ L of propidium iodide (20 μ g/mL) to the binding buffer. The results of apoptosis were detected by flow cytometry within 1 h.

Statistical analysis

All results are presented as the mean \pm SD. Statistical analysis was performed using GraphPad Prism 5.0. An independent sample t-test was used for comparison between two groups at the same time point, and two-way ANOVA was used for comparison between two groups at multiple time points. A value of $p < 0.05$ was considered statistically significant. In all figures, we used * to denote p -values, in which * $p < 0.05$, ** $p < 0.01$, *** $p < 0.001$, **** $p < 0.0001$ and no significance $p > 0.05$.

Results

PRP promoted skin wound healing

To investigate the effect of PRP on skin wound healing, a full-thickness skin defect model was used and wound healing progress was analyzed at different time points after skin injury. The results showed that compared with the control group, the wound closure of the PRP group was significantly accelerated, and the wound was clean with much less exudation (Figure 1a, b). These results were further confirmed by H&E staining (Figure 1c).

PRP was involved in decreasing the wound inflammatory response

An inflammatory response is the initial step in the process of wound healing, and a moderate inflammatory reaction is helpful to normal wound healing [13]. To evaluate the effect of PRP on wound inflammation, we analyzed the inflammatory cell infiltration and cytokine expression in wound tissues of animals with or without PRP treatment. By means of H&E

staining, we observed that inflammatory cell infiltration was decreased slightly in the PRP group (Figure 2a), but there was no significant difference between the two groups (Figure 2b).

Due to the critical roles of IL-1 β , IL-23, IL-17 and TNF- α in inflammation [14], we further examined the expression of these inflammatory factors in wound tissues by means of immunohistochemistry. The positive expression of IL-1 β , IL-23, IL-17 and TNF- α were mainly present in the area of granulation tissue and panniculus carnosus below the wound (Figure 2c). Among these inflammatory cytokines, the production of IL-17 and IL-1 β , but not IL-23 and TNF- α , were significantly decreased in wound tissues from the PRP group compared with the control group (Figure 2d).

PRP significantly promoted angiogenesis of wound tissue

Granulation tissue is essential for effective wound healing. The formation of granulation tissue in the early stage provides a nutritional environment for wound repair, and effective absorption in the later stage can prevent the formation of scar tissue [15]. Therefore, we evaluated the granulation tissue at the wound site in both groups. We found that granulation tissue was obvious in the PRP group on day 5, and inflammatory cells and vascular infiltration were increased relative to the control group. The granulation tissue was almost totally absorbed on day 7, and the PRP promoted the absorption of granulation without causing loss of its organization (Figure 3a, b).

Angiogenesis plays critical roles in effective wound healing [16]. To evaluate the effect of PRP on angiogenesis, we examined neovascularization in wound tissue on days 5 and 7 after skin injury by means of H&E staining. The results showed that the amount of neovascularization, which was mainly distributed below the wound margin and in the granulation tissue, was significantly increased in the wound tissues of the PRP group compared with the control group (Figure 3c, d).

To further confirm the positive impact of PRP on angiogenesis, we detected the expression of CD31 [17], a marker for evaluating vascularization and angiogenesis, and VEGF, a crucial growth factor for vascular endothelial cell division and angiogenesis in wound tissue [18]. The results showed that, compared to the control group, the number of CD31 positive cells was significantly increased in wound tissues of the PRP group, especially on day 5 after injury (Figure 3e, f). Consistent with the results of CD31 expression, PRP treatment also enhanced VEGF production in the wound tissues, suggesting that PRP had a positive impact on angiogenesis by enhancing the production of VEGF in wound tissue (Figure 3g, h).

PRP promoted wound contraction and stabilized the collagen arrangement

Wound contraction can effectively reduce the wound area and shorten healing time. To detect the effect of PRP on wound contraction, we measured the linear distance between the panniculus carnosus of the wound on the third, fifth and seventh day after injury. By means of IPP measurement,

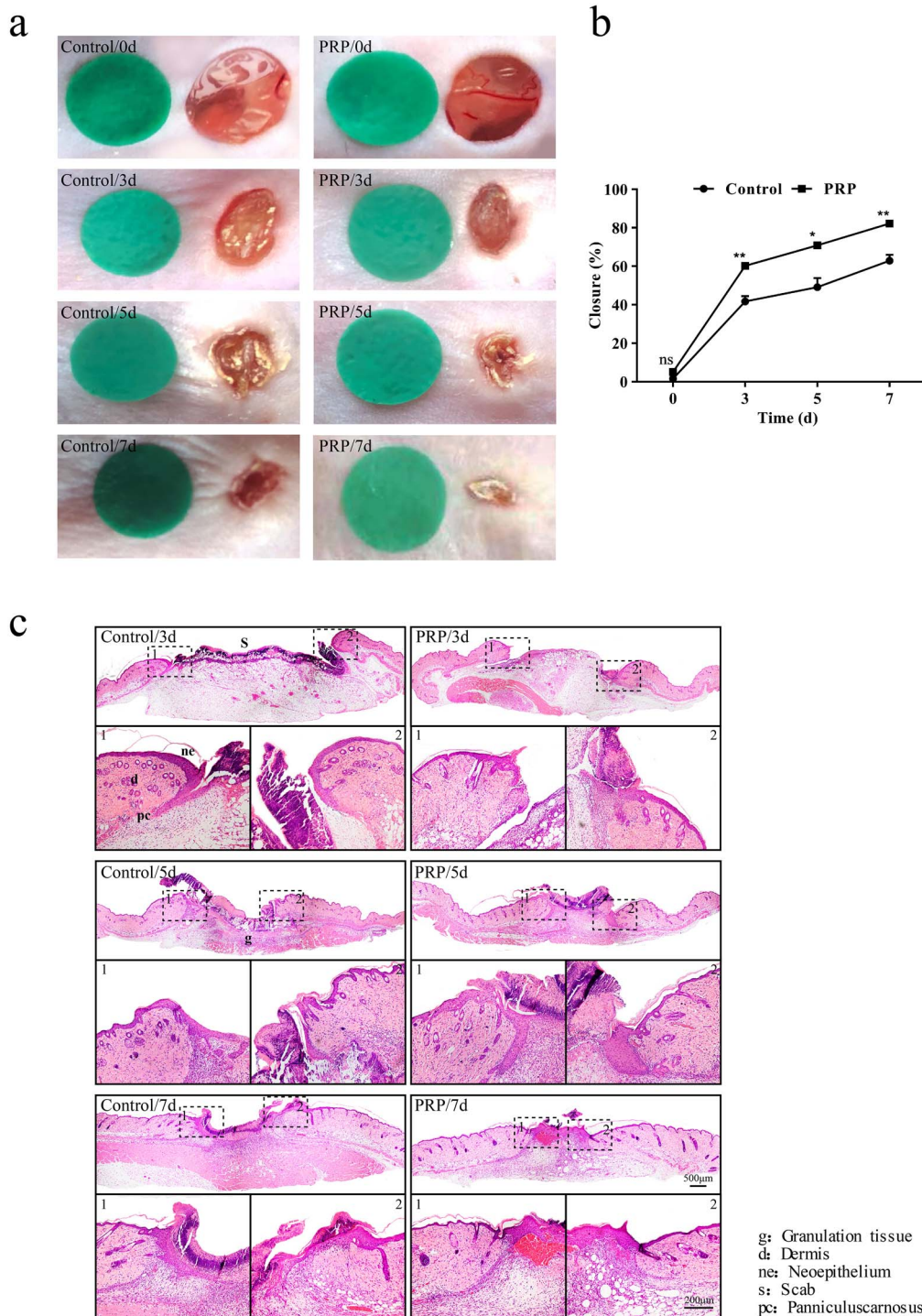


Figure 1. Gross view and morphological observations in the control and PRP treated groups. (a) Sequential photographs of skin wounds in mice treated with saline and PRP at different time points (days 3, 5 and 7 after injection). Compared with the control group, PRP significantly promoted closure with a clean wound with less exudate. (b) Calculation and comparison of the closure rate of each group at different time points on days 3, 5 and 7 after injection. Non-healed area of the PRP group was ~18%, and the difference was statistically significant compared with the control, $p < 0.05$. Data are presented as the mean \pm SD ($n=5$). Statistical analysis: ** $p < 0.01$, * $p < 0.05$. ns $p > 0.05$. (c) Representative histologic analysis of the wound region. Tissue samples were collected on days 3, 5 and 7 after injection. Hematoxylin and eosin (H&E) staining showed wound healing and re-epithelialization in the PRP group was better than in the control group. Scale bar = 500 μ m. Local magnification of the areas surrounded by dashed black boxes shows that the neo-epidermis thickness was increased and the tissue structure was clear after treatment with PRP. Scale bar = 200 μ m. PRP platelet-rich plasma, ns no significance

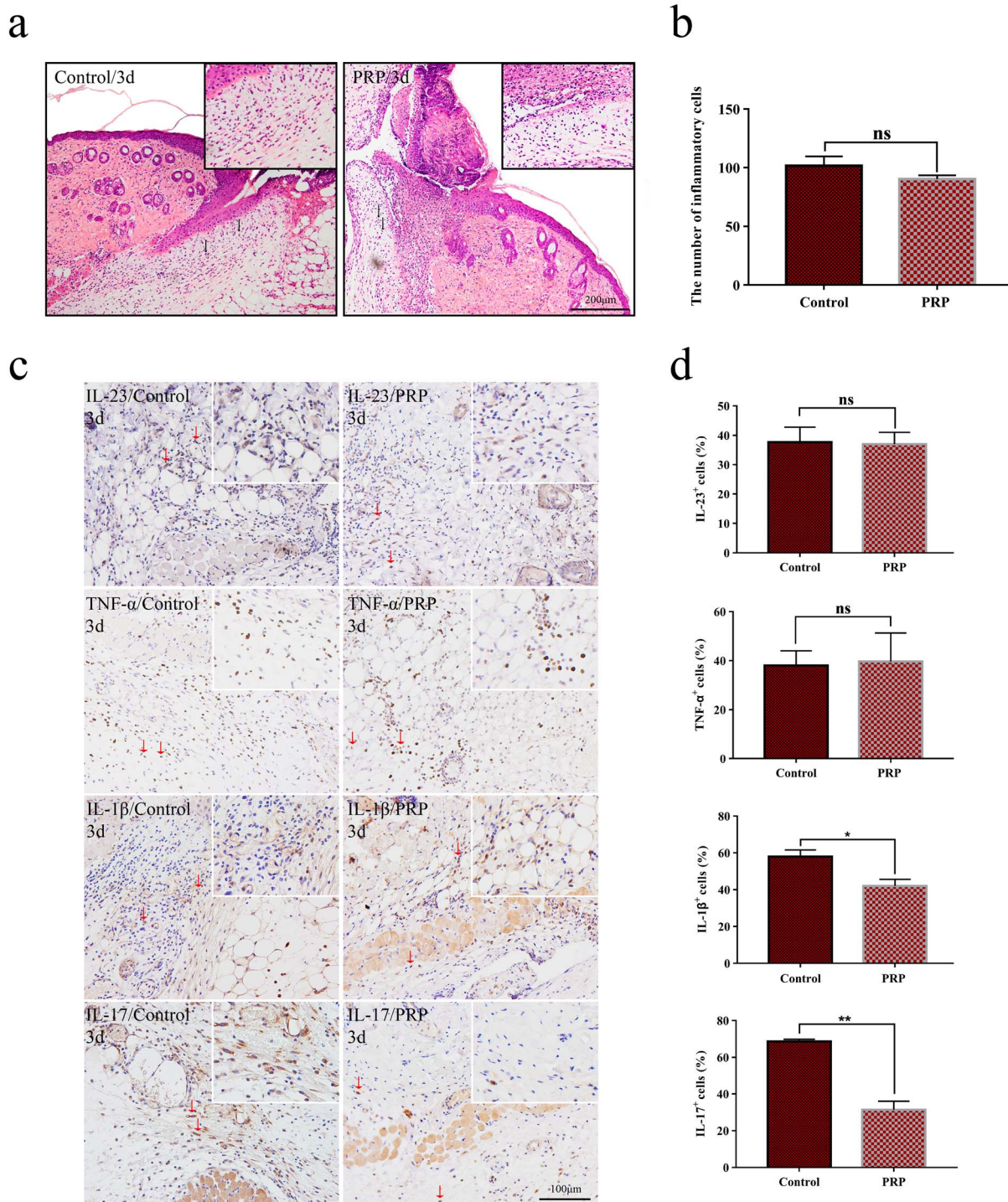


Figure 2. Observation of inflammatory infiltration of wounds in the control and PRP treated groups. (a) Hematoxylin and eosin (H&E) staining of inflammatory cells in mice treated with saline and PRP on day 3 after injection. Red arrows indicate inflammatory cell infiltrates. Scale bar = 200 μ m. (b) Statistical analysis of inflammatory infiltrating cells. There was no significant difference between the two groups with $p > 0.05$. Data are presented as the mean \pm SD ($n = 5$). Statistical analysis: ns $p > 0.05$. (c) The expression of interleukin-23 (IL-23), tumor necrosis factor- α (TNF- α), interleukin-1 β (IL-1 β) and interleukin-17 (IL-17) in PRP and control groups on day 3 by immunohistochemical methods. Red arrows indicate positive cell infiltrates. Scale bars = 100 μ m. (d) Calculation and comparison of the positive cells of each group on day 3. IL-1 β and IL-17 were significantly decreased in the PRP group compared with the control group, while the expression of IL-23 and TNF- α was not significantly different between the two groups. Data are presented as the mean \pm SD ($n = 5$). Statistical analysis: ** $p < 0.01$, * $p < 0.05$. ns $p > 0.05$. PRP platelet-rich plasma, ns no significance

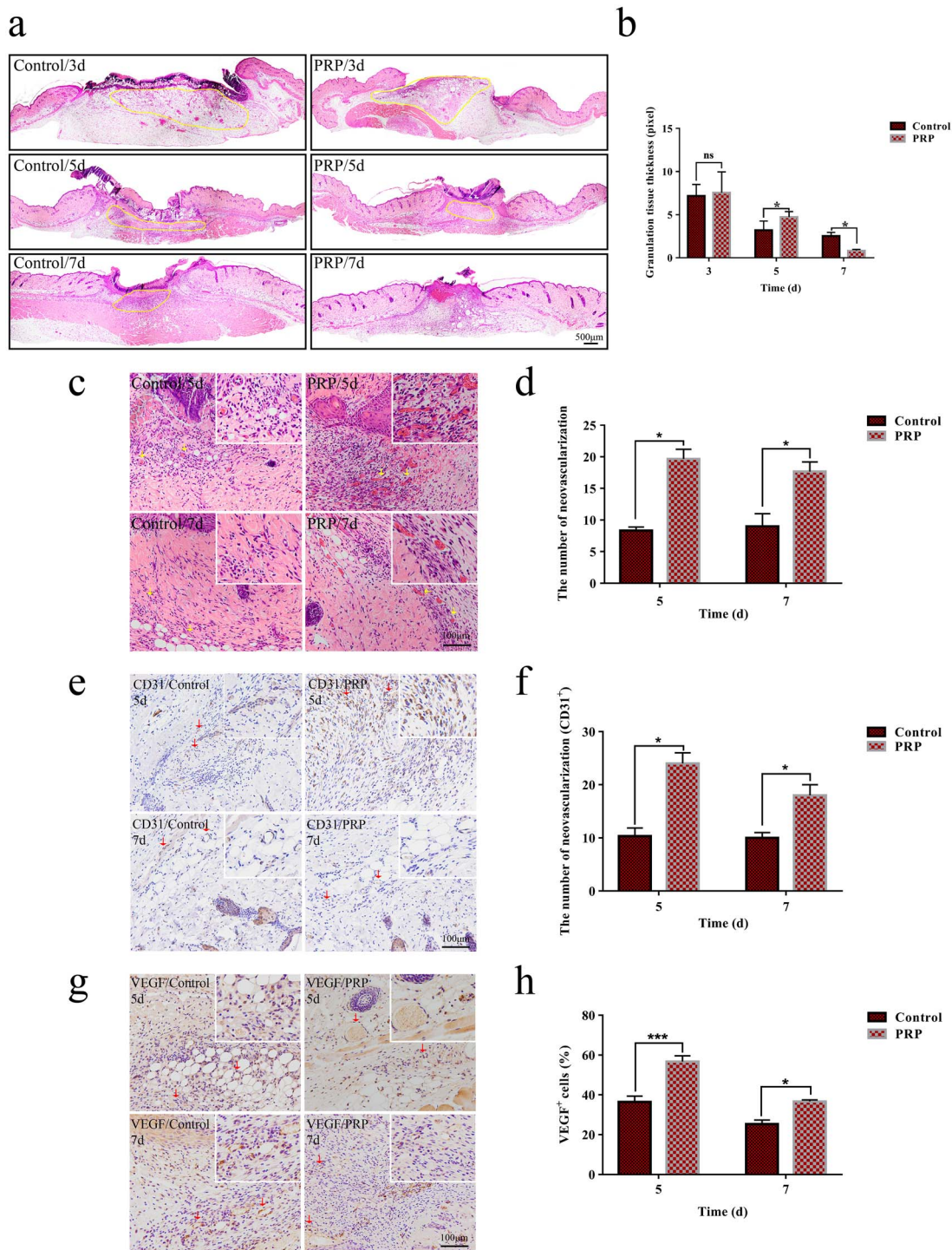


Figure 3. Angiogenesis and granulation tissue formation in the control and PRP treated groups. (a) Hematoxylin and eosin (H&E) staining showing the granulation tissue in the PRP and control groups on days 3, 5 and 7 after injection. The granulation tissue of the PRP group was homogeneous with an internal visible vascular network arrangement. Compared with the control, the granulation tissue was gradually replaced by tissue remodeling in the PRP group, as shown in the yellow area. Scale bar = 500 μ m. (b) Quantitative analysis of granulation tissue in the two groups with Image-Pro Plus (IPP) software. There were significant differences between the two groups on days 5 and 7. Data are presented as the mean \pm SD (n=5). Statistical analysis: * p < 0.05. ns p > 0.05. (c) H&E staining analysis of angiogenesis in the PRP and control group on days 5 and 7. Yellow arrows indicated neovascularization in the two groups. Neovascularization was scattered around the wound with different sizes. Scale bar = 100 μ m. (d) The statistical results of neovascularization showed that the amount in the PRP group was larger than that of the control group, and the difference was statistically significant on days 5 and 7. Data are presented as the mean \pm SD (n=5). Statistical analysis: * p < 0.05. (e, g) The expression of platelet endothelial cell adhesion molecule-1 (CD31) and vascular endothelial growth factor (VEGF) in the PRP and control group on days 5 and 7 with immunohistochemical methods. Red arrows indicate the positive cells in the two groups. The scale bar = 100 μ m. (f, h) Statistical analysis of positive cells of each group on days 5 and 7. The expression of CD31 and VEGF in the PRP group were significantly higher than that in the control group. Data are presented as the mean \pm SD (n=5). Statistical analysis: *** p < 0.001, * p < 0.05. PRP platelet-rich plasma, ns no significance

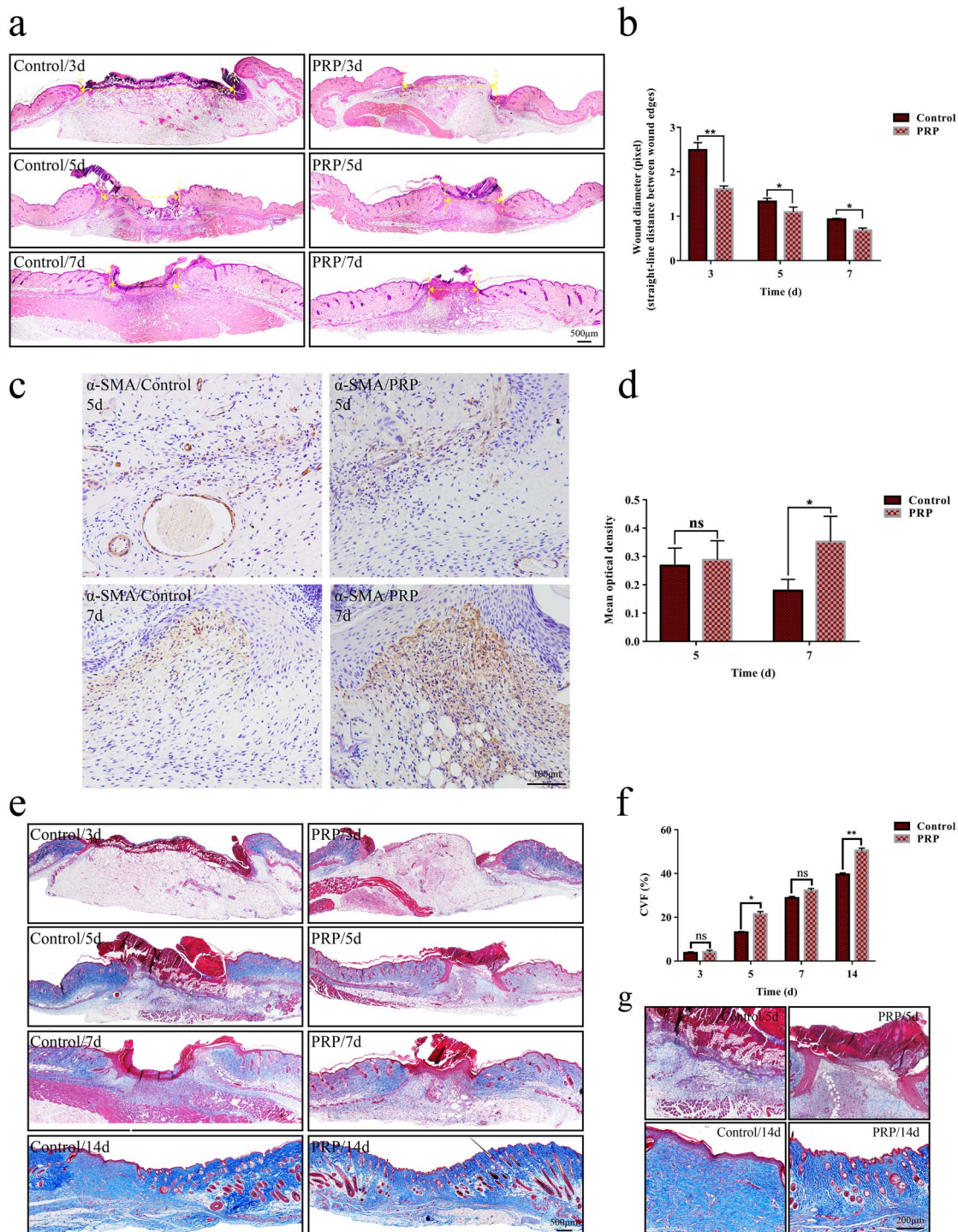


Figure 4. Wound contraction and collagen deposition in the control and PRP treated groups. **(a)** Wound contraction is represented by the vertical distance between the margins of the wound, as shown by the yellow double-headed arrow. This showed that the distance in the PRP group was shorter than that in the control group. Scale bar = 500 μ m. **(b)** The distance was measured by Image-Pro Plus (IPP) software, and the statistical results showed that there was a significant difference between the two groups on days 3, 5 and 7 after injection. Data are presented as the mean \pm SD (n=5). Statistical analysis: ** $p < 0.01$, * $p < 0.05$. **(c)** Immunohistochemical staining with α -smooth muscle actin (α -SMA) in the PRP and control group on days 5 and 7. Positive signals around the wound can be seen, extending to the center of the wound, as shown in the brown area. Scale bar = 100 μ m. **(d)** Statistical analysis of positive signals showed that the secretion of α -SMA in the PRP group was more than that in control group on day 7. Data are presented as the mean \pm SD (n=5). Statistical analysis: * $p < 0.05$. ns $p > 0.05$. **(e)** Masson's trichrome staining indicated the collagen deposition in the wounds in the PRP and control group on days 3, 5, 7 and 14. The deposition of collagen was significantly greater in the PRP group than that in the control group on days 5 and 14. Scale bar = 500 μ m. **(f)** The collagen volume fraction (CVF) was measured by IPP, and the statistical results showed that there was a significant difference between the two groups on days 5 and 14. Data are presented as the mean \pm SD (n=5). Statistical analysis: ** $p < 0.01$, * $p < 0.05$, $p > 0.05$. **(g)** Local magnification of collagen deposition in the wound on days 5 and 14. Collagen deposition in the PRP group was greater than that in the control group and arranged neatly, which was similar to normal skin, and meanwhile the regeneration of skin appendages can be seen. Scale bar = 200 μ m. PRP platelet-rich plasma, ns no significance

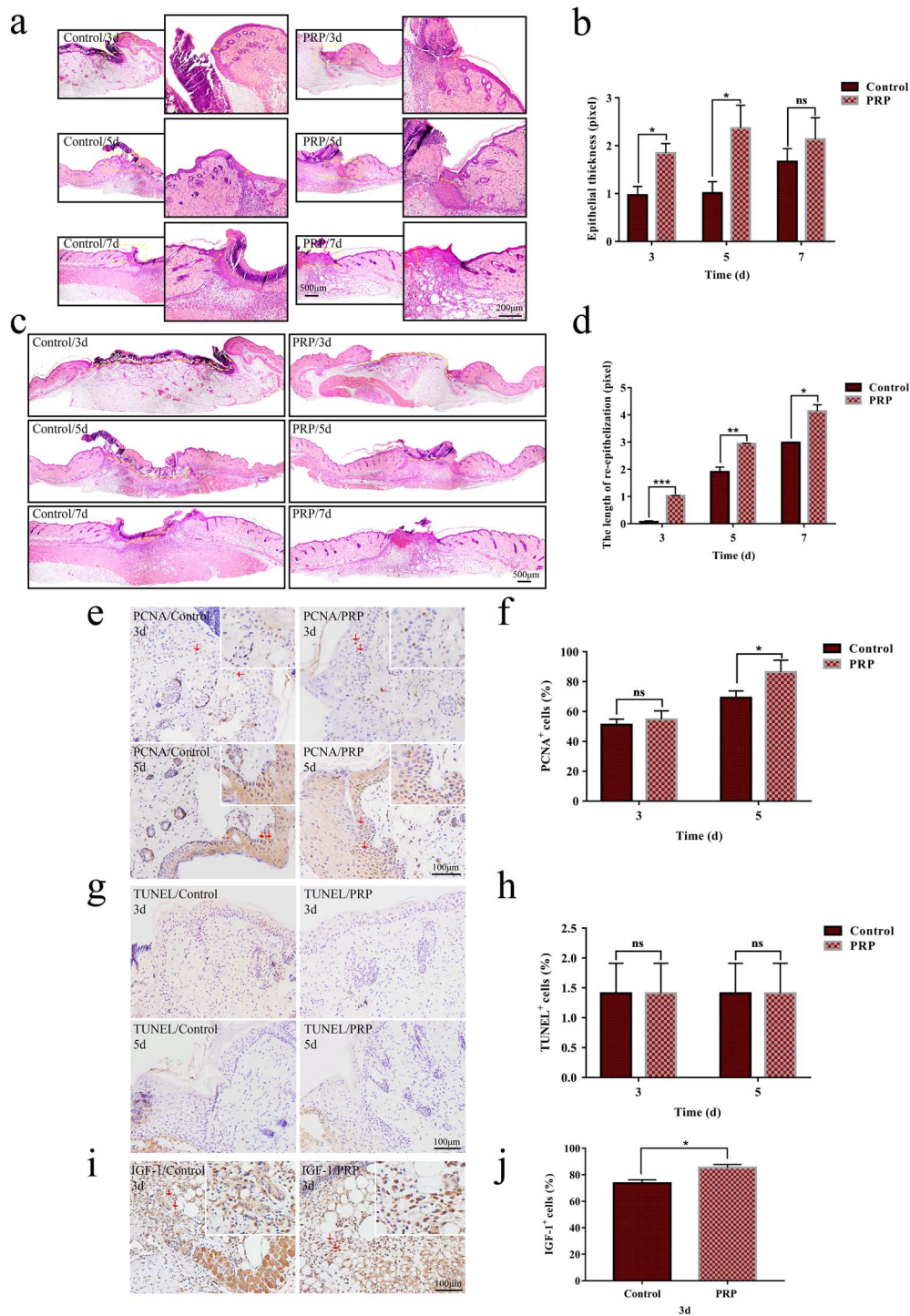


Figure 5. Evaluation of re-epithelialization in the control and PRP treated groups. (a,c) Hematoxylin and eosin (H&E) staining analysis of regenerated skin tissue in the PRP and control groups on days 3, 5 and 7 after injection. (a) The change of thickness of the neo-epidermis, as shown by the yellow arrow in the local magnification; (c) the change in the length of the neo-epithelial tongue, and the yellow dotted line represents the unhealed length. Scale bars = 200 μ m and 500 μ m, respectively. (b,d) Statistical analysis of neo-epidermis thickness and neo-epithelial tongue length shows that there was a statistically significant difference between the two groups on days 3, 5 and 7. Data are presented as the mean \pm SD (n=5). Statistical analysis: *** $p < 0.001$, ** $p < 0.01$, * $p < 0.05$. ns $p > 0.05$. (e,g) Immunohistochemical staining of proliferating cell nuclear antigen (PCNA) and TUNEL in the PRP and control group on days 3 and 5. The infiltration of positive cells can be seen at the neo-epidermis site, as shown by the brown signal. Scale bar = 100 μ m. (f,h) Statistical results of the number of positive cells. Compared with the control group, the number of PCNA positive cells in the PRP group increased significantly, while there was no significant difference for apoptotic cells. Data are presented as the mean \pm SD (n=5). Statistical analysis: * $p < 0.05$. ns $p > 0.05$. (i) The immunohistochemical staining with insulin-like growth factor-1 (IGF-1) in the PRP and control group on day 3. The positive cells of IGF-1 in the PRP group were more than that in the control group, as shown by the brown histograms. Scale bar = 100 μ m. (j) Statistical results of IGF-1 expression. The expression of positive cells was significantly increased in the PRP group. Data are presented as the mean \pm SD (n=5). Statistical analysis: * $p < 0.05$. PRP platelet-rich plasma, ns no significance

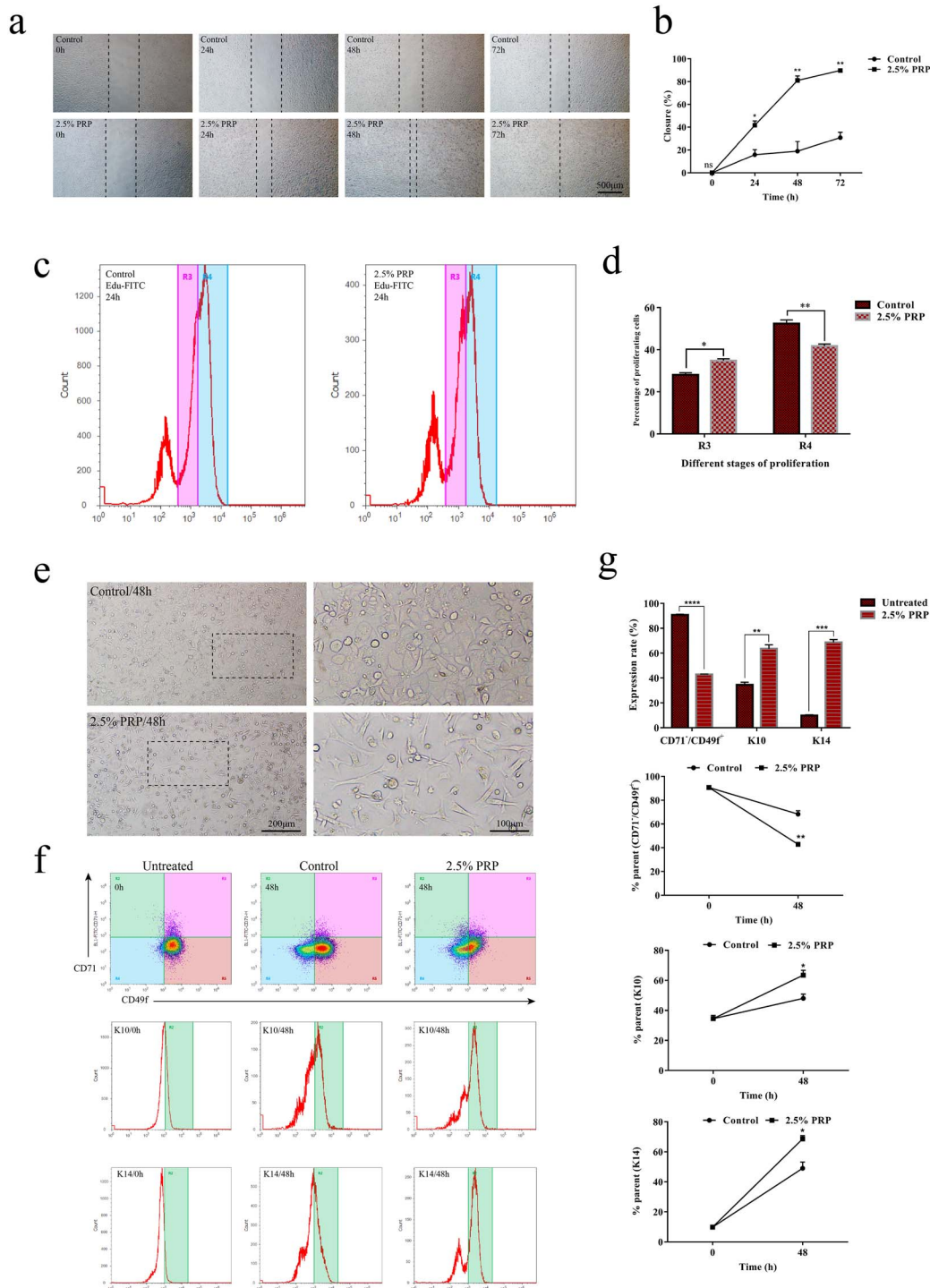


Figure 6. The effect of platelet-rich plasma (PRP) on the biological function of epidermal stem cells (ESCs). (a) Microscopic images of scratch of ESCs at 0, 24, 48 and 72 h, respectively, with or without treatment with 2.5% PRP. Untreated cells were taken as the control. PRP significantly promoted the migration ability of epidermal stem cells, with the scratch at 72 h having basically healed but not in the control group. Scale bar = 500 μm. (b) Calculated scratch migration rate of ESCs. PRP promoted ESCs migration, and the difference was statistically significant relative to the control. Data are presented as the mean ± SD (n=3). Statistical analysis: ** $p < 0.01$, * $p < 0.05$, ns $p > 0.05$. (c) Analysis of the proliferation ability of ESCs by EdU flow detection. R4 represents the mother generation and R3 represents the offspring generation. The number of R4 in the PRP group was lower, while the number of R3 was increased relative to the control group after treatment with PRP for 24 h. (d) Calculation and comparison of proliferating cells at 24 h, the difference was statistically significant between PRP and the control group. Data are presented as the mean ± SD (n=3). Statistical analysis: ** $p < 0.01$, * $p < 0.05$. (e) Microscopic images of ESCs after treatment with 2.5% PRP for 48 h. The cells in the PRP group showed a differentiation phenotype with a dendritic shape. The nuclear/cytoplasmic ratio decreased. Scale bars = 200 and 100 μm. (f) The expression of CD71-CD49f+, and keratin 14/keratin 10 (K14/K10) by flow cytometry after treatment with 2.5% PRP for 48 h. The untreated group (0 h) represents the initial state of the PRP and control groups. The expression of CD49f decreased significantly, while the expression of K10 and K14 were increased relative to the control and untreated group. (g) Data analysis showed that the difference was statistically significant between the control and untreated group. Statistical analysis: **** $p < 0.0001$, *** $p < 0.001$, ** $p < 0.01$, * $p < 0.05$. ns no significance

we observed that PRP could markedly shorten the distance between the panniculus carnosus, suggesting that PRP facilitated wound contraction. (Figure 4a, b).

Myofibroblasts are the key cells to induce wound contraction, so we further evaluated the effect of PRP on myofibroblast formation by detecting the expression of the myofibroblast marker α -smooth muscle actin (α -SMA) in wound tissues. The results showed that PRP could enhance the production of α -SMA in wound tissues and increase the number of α -SMA positive cells, suggesting that PRP could promote the formation of wound myofibroblasts (Figure 4c, d).

The expression and arrangement of collagen fibers in the wound determine the quality of tissue remodeling [16]. For this reason, we evaluated the effect of PRP on collagen formation in wound tissues by the Masson trichromatic method. The results showed collagen deposition under the wound was significantly increased (Figure 4e, f), accompanied by an ordered arrangement and uniform density (Figure 4g), in the PRP group compared with the control group. This suggested that PRP could provide a favorable environment for further tissue remodeling.

PRP promoted re-epithelialization

Re-epithelialization is one of the key steps in the process of skin wound repair [16]. PRP significantly increased the thickness and length of the neo-epithelial tongue on days 3, 5 and 7 after skin injury (Figure 5a–d). Since epidermal cells are the cellular basis of re-epithelialization, we further evaluated the effect of PRP on the proliferation and apoptosis of neo-epidermal tissue by PCNA staining and TUNEL assays. The results showed that PRP treatment markedly increased the proliferation (Figure 5e, f), but had no significant impact on apoptosis of the neo-epidermal tissue (Figure 5g, h). These results indicated that PRP might promote re-epithelialization by increasing the proliferation, but not reducing the apoptosis, of epidermal cells. Furthermore, we detected the expression of IGF-1, an important growth factor for epidermal cell proliferation, in wound tissue. The results showed that, compared to the control group, the number of IGF-1 positive cells was significantly increased on day 3 in wound tissues of the PRP group (Figure 5i, j), suggesting that PRP promotes the production of IGF-1 in wound tissues in early stages of skin injury.

PRP regulated the biological function of ESCs

The proliferation, differentiation and migration of ESCs is the cellular basis of the re-epithelialization process [19]. To clarify the underlying mechanism of PRP-mediated promotion of re-epithelialization, we investigated the effect of PRP on the proliferation, differentiation and migration of ESCs *in vitro*.

We successfully isolated primary ESCs and examined the effect of PRP on their survival (see online supplementary material). First, we checked the effects of PRP on the proliferation of ESCs by means of EdU assays. The results showed that, compared with the control group, the proliferation and

division of ESCs was significantly increased in the PRP group, accompanied by dendrites type changes (Figure 6c, d).

Then, we detected the effect of PRP on the differentiation of ESCs by means of flow cytometry. The results showed that ESCs treated with PRP expressed lower levels of CD49f and higher levels of K14 and K10 (Figure 6e–g).

Finally, we examined the impact of PRP on the migration of ESCs by means of scratch assays. The results showed that, compared with the control group, the migration of ESCs was significantly enhanced in the PRP group (Figure 6a, b). These results demonstrated that PRP could promote re-epithelialization by enhancing the proliferation, differentiation and migration of ESCs.

Discussion

PRP has been reported to be able to promote skin wound healing and it is widely used in the clinical treatment of patients suffering from chronic wounds. Wound inflammation, angiogenesis, wound contraction and re-epithelialization are the four critical factors in skin wound repair [20]. However, a systematic evaluation of the impact of PRP on these factors has been lacking. Here, we demonstrated that the positive effects of PRP on re-epithelialization, wound inflammation, angiogenesis and wound contraction coordinately contributed to promote skin wound repair.

Re-epithelialization is required for efficient skin wound closure. Researchers previously found that PRP treatment accelerated the re-epithelialization and epidermal differentiation of acute wounds in dogs [21, 22]. Similar results were observed in our study. The re-epithelialization of wounds could be significantly enhanced by PRP, which could markedly increase the thickness and length of the neo-epidermal tissue.

Re-epithelialization results from the proliferation and differentiation of epidermal cells, in which multiple growth factors, including VEGF [23], epidermal growth factor (EGF) [24, 25], FGF [25, 26], TGF- β [27, 28], PDGF [29] and IGF-1 [30] play critical roles. It has been reported that PRP can induce tissue cells to produce these factors through autocrine or paracrine mechanisms, especially EGF and TGF- β . Among these factors, IGF-1 has been demonstrated to be important for the growth, maintenance and repair of skin tissues. Some studies have found that PRP could increase the expression of IGF-1 in *in situ* injuries, such as OA and nerve injury [31–33]. Similarly, our results showed that PRP enhanced the production of IGF-1 in wound tissues, suggesting that IGF-1 contributed to PRP-mediated promotion of re-epithelialization.

ESCs play crucial roles in the proliferation and differentiation of epidermal cells and are required for efficient re-epithelialization [34]. When a wound occurs, ESCs quickly form clones at the wound base and then expand to the wound center, gradually differentiating into daughter cells to fill the skin tissue defect [19, 35]. It has been reported that platelet-rich gel could promote the differentiation and proliferation of ESCs in a model of New Zealand white rabbit burn

wounds [36]. In that study, $\beta 1$ integrin and p63 were used as biomarkers for the differentiation of ESCs. To confirm the effects of PRP on the differentiation of ESCs, we used two biomarker systems, CD71/CD49f and K14/K10, to define ESCs, TAC and PMD. In line with previous studies, our data demonstrated that PRP could effectively promote the proliferation of ESCs, and promote the differentiation of ESCs into TAC and PMD. Furthermore, we revealed that PRP could also significantly promote the migration of ESCs. Combined with our *in vivo* results, it is reasonable to assume that PRP enhances the proliferation, differentiation and migration of ESCs to promote re-epithelialization, in which the IGF-1/IGF-1R pathway might be involved.

The inflammatory response is the first wound defense mechanism and is essential to the whole healing process [37]. There is a balance between anti-inflammatory and pro-inflammatory signals in inflammatory responses, and moderate inflammation is beneficial, but excessive inflammation is harmful, to tissue repair [38]. PRP was reported to regulate inflammation by reducing the levels of IL-17/IL-1 β in patients with OA to a certain extent and improve their pain symptoms and joint function [39]. Consistent with the results of previous studies, we observed that PRP decreased the extent of wound inflammation. Our data showed that, although there was only a slight impact on infiltration of inflammatory cells into wound tissues, PRP treatment could significantly reduce the production of IL-17A and IL-1 β in wound tissues. This suggested that PRP has a capacity for regulating wound inflammation, which contributes to the improvement of skin wound repair.

The formation of blood vessels from the surrounding edges provides the necessary nutrients and oxygen for wound healing [40]. The quality and quantity of neovascularization determine the quality of wound healing. As a specific heparin-binding growth factor for vascular endothelial cells, VEGF promotes endothelial cell proliferation and angiogenesis by binding to the corresponding receptors on the vascular endothelium, reflecting the ability of wound angiogenesis [41,42]. It has been reported that PRP could promote angiogenesis after burns and trauma by promoting the proliferation of endothelial cells and the expression of VEGF. We also found that PRP could promote the effective secretion of VEGF in wound tissue and increase the amount of neovascularization around the wound, further confirming the positive impact of PRP on angiogenesis.

Damage to or the absence of skin appendages not only delays wound healing but also leads to incomplete skin function and scar outcomes [43]. There have been clinical cases of PRP used in the treatment of alopecia [44, 45], and further in-depth research found that it could affect the hair growth cycle and is beneficial to hair follicle reconstruction [46, 47]. Interestingly, the hair follicles and sebaceous glands were distributed in the newborn skin in the PRP group on day 14, which is consistent with previous research. PRP promotes the regeneration of skin appendages, which may provide more possibilities for the clinical treatment of severe burn

trauma. Its application in skin hair follicle regeneration has great prospects and value.

Another important stage of wound healing is wound contraction and collagen deposition. Effective wound contraction is beneficial to shorten the healing time, while the deposition and orderly arrangement of collagen fibers in the wound reduces the possibility of scar repair, which is beneficial to improve the quality of tissue remodeling [48, 49]. Many studies of PRP promoting wound healing have shown that the use of PRP alone or combined with biomaterial scaffolds can promote collagen deposition and effectively shorten healing time [21, 50]. We also reached the same conclusion in our study. Myofibroblasts are thought to play an important role in wound contraction. In the middle and late stages, the differentiation of fibroblasts into myofibroblasts gradually increased with the formation of granulation tissue, which will drive the effective contraction of the wound margin [51, 52]. Previous studies found that PRP treatment for wound healing resulted in a greater proportion of myofibroblasts present at the wound site by quantifying α -SMA, specifically expressed by myofibroblasts [53]. In our study, PRP could increase the secretion of α -SMA, the same as in the previous study. This is a key point for PRP to promote contraction and wound healing.

Conclusions

In summary, we performed the first comprehensive analysis of the effect of PRP on wound healing in a basic experiment, which further identified a key role of PRP in the three important stages of wound healing. This facilitation is multifaceted. It strongly enhances re-epithelialization, induces angiogenesis and is also involved in wound contraction and collagen deposition. Although there are still some molecular mechanisms to be explored in depth, our study supports the use of PRP as an adjuvant to boost wound healing.

Abbreviations

bFGF: basic fibroblast growth factor; BMSC: bone marrow stromal cells; ECS: epidermal stem cell; H&E: hematoxylin and eosin; IGF-1: insulin-like growth factor-1; IL-23: interleukin 23; IL-1 β : interleukin 1 β ; IL-17: interleukin 17; IPP: Image-Pro Plus; K10: keratin 10; OA: osteoarthritis; PBS: phosphate buffer saline; PCNA: proliferating cell nuclear antigen; PDGF: platelet-derived growth factor; PMD: post-mitotic differentiating cell; PRP: platelet-rich plasma; α -SMA: α -smooth muscle actin; TAC: transit amplifying cell; TGF- β , transforming growth factor- β ; TNF- α : tumor necrosis factor α ; VEGF: vascular endothelial growth factor.

Supplementary data

Supplementary data is available at *Burns & Trauma Journal* online.

Authors' contributions

PX wrote the manuscript. PX, WH and BC designed the research. PX, YW, LZ and ZY performed animal experiment of wound healing. PX, XZ, XH, JY, MW and BW performed immunohistochemistry microscopy, cell function assay. PX, WH and BC analyzed the data. WH participated in critically revising the article. GL supervised the study. All authors read and approved the final manuscript.

Funding

This work was supported by the National Key Research and Development Plan of China (No.2017YFC1103301), and Military Medical Innovation Special Projects (No. 18CXZ029), National Natural Science Foundation of China (31872742), Top-notch Talent Training Plan (SWH2018BJKJ-04), Military Medical Science and Technology Youth Training Plan (20QNPHY024).

Availability of data and materials

All data generated and/or analyzed during the current study are included in this published article.

Ethics approval

All animal experiments were approved by the Medical and Ethics Committee of Southwest Hospital, Third Military Medical University (Army Medical University), Chongqing, China.

Conflict of Interest

The authors declared that they have no conflicts of interest to this work.

References

- Marx RE. Platelet-rich plasma: evidence to support its use. *J Oral Maxillofac Surg.* 2004; 62(4): 489–96.
- Chicharro-Alcantara D, Rubio-Zaragoza M, Damiá-Giménez E, Carrillo-Poveda JM, Cuervo-Serrato B, Peláez-Gorrea P, et al. Platelet rich plasma: new insights for cutaneous wound healing management. *J Funct Biomater.* 2018; 9(1): 10.
- Eppley BL, Woodell JE, Higgins J. Platelet quantification and growth factor analysis from platelet-rich plasma: implications for wound healing. *Plast Reconstr Surg.* 2004; 114(6): 1502–8.
- Ozer K, Colak O. Leucocyte- and platelet-rich fibrin as a rescue therapy for small-to-medium-sized complex wounds of the lower extremities. *Burns Trauma.* 2019; 7: 11 doi: [10.1186/s41038-019-0149-0](https://doi.org/10.1186/s41038-019-0149-0).
- Sun Y, Cao Y, Zhao R, Xu F, Wu D, Wang Y. The role of autologous PRP on deep partial-thickness burn wound healing in Bama pigs. *J Burn Care Res.* 2020; 41(3): 657–62.
- Lian Z, Yin X, Li H, Jia L, He X, Yan Y, et al. Synergistic effect of bone marrow-derived mesenchymal stem cells and platelet-rich plasma in streptozotocin-induced diabetic rats. *Ann Dermatol.* 2014; 26(1): 1–10.
- Wang B, Geng Q, Hu J, Shao J, Ruan J, Zheng J. Platelet-rich plasma reduces skin flap inflammatory cells infiltration and improves survival rates through induction of angiogenesis: an experiment in rabbits. *J Plast Surg Hand Surg.* 2016; 50(4): 239–45.
- Chai J, Ge J, Zou J. Effect of autologous platelet-rich plasma gel on skin flap survival. *Med Sci Monit.* 2019; 25: 1611–20.
- Zhang W, Guo Y, Kuss M, Shi W, Aldrich AL, Untrauer J, et al. Platelet-rich plasma for the treatment of tissue infection: preparation and clinical evaluation. *Tissue Eng Part B Rev.* 2019; 25(3): 225–36.
- Elsaid A, El-Said M, Emile S, Youssef M, Khafagy W, Elshobaky A. Randomized controlled trial on autologous platelet-rich plasma versus saline dressing in treatment of non-healing diabetic foot ulcers. *World J Surg.* 2020; 44(4): 1294–301.
- Volakakis E, Papadakis M, Manios A, Ioannou CV, Zoras O, de Bree E. Platelet-rich plasma improves healing of pressure ulcers as objectively assessed by digital Planimetry. *Wounds.* 2019; 31(10): 252–6.
- Evans A, Ibrahim M, Pope R, Mwangi J, Botros M, Johnson SP, et al. Treating hand and foot osteoarthritis using a patient's own blood: a systematic review and meta-analysis of platelet-rich plasma. *J Orthop.* 2020; 18: 226–36.
- Eming SA, Martin P, Tomic-Canic M. Wound repair and regeneration: mechanisms, signaling, and translation. *Sci Transl Med.* 2014; 6(265): 265sr6.
- Larouche J, Sheoran S, Maruyama K, Martino MM. Immune regulation of skin wound healing: mechanisms and novel therapeutic targets. *Adv Wound Care (New Rochelle).* 2018; 7(7): 209–31.
- Alhaji M, Bansal P, Goyal A. *Physiology, Granulation Tissue. Treasure Island (FL).* StatPearls Publishing, 2020, 01.
- Gurtner GC, Werner S, Barrandon Y, Longaker MT. Wound repair and regeneration. *Nature.* 2008; 453(7193): 314–21.
- Li ZJ, Wang ZZ, Zheng YZ, Xu B, Yang RC, Scadden DT, et al. Kinetic expression of platelet endothelial cell adhesion molecule-1 (PECAM 1/CD31) during embryonic stem cell differentiation. *J Cell Biochem.* 2005; 95(3): 559–70.
- Peng Y, Wu S, Li Y, Crane JL. Type H blood vessels in bone modeling and remodeling. *Theranostics.* 2020; 10(1): 426–36.
- Senoo M. Epidermal stem cells in homeostasis and wound repair of the skin. *Adv Wound Care (New Rochelle).* 2013; 2(6): 273–82.
- Singer AJ, Clark RA. Cutaneous wound healing. *N Engl J Med.* 1999; 341(10): 738–46.
- Jee CH, Eom NY, Jang HM, Jung HW, Choi ES, Won JH, et al. Effect of autologous platelet-rich plasma application on cutaneous wound healing in dogs. *J Vet Sci.* 2016; 17(1): 79–87.
- Farghali HA, AbdElKader NA, Khatib MS, AbuBakr HO. Evaluation of subcutaneous infiltration of autologous platelet-rich plasma on skin-wound healing in dogs. *Biosci Rep.* 2017; 37(2): BSR20160503. doi: [10.1042/BSR20160503](https://doi.org/10.1042/BSR20160503).
- Bao P, Kodra A, Tomic-Canic M, Golinko MS, Ehrlich HP, Brem H. The role of vascular endothelial growth factor in wound healing. *J Surg Res.* 2009; 153(2): 347–58.
- Brown GL, Nanney LB, Griffen J, Cramer AB, Yancey JM, Curtsinger LJ, et al. Enhancement of wound healing by topical treatment with epidermal growth factor. *N Engl J Med.* 1989; 321(2): 76–9.
- Choi SM, Lee KM, Kim HJ, Park IK, Kang HJ, Shin HC, et al. Effects of structurally stabilized EGF and bFGF on wound

- healing in type I and type II diabetic mice. *Acta Biomater.* 2018; 66: 325–34.
26. Xie J, Bian H, Qi S, Xu Y, Tang J, Li T, *et al.* Effects of basic fibroblast growth factor on the expression of extracellular matrix and matrix metalloproteinase-1 in wound healing. *Clin Exp Dermatol.* 2008; 33(2): 176–82.
 27. Le M, Naridze R, Morrison J, Biggs LC, Rhea L, Schutte BC, *et al.* Transforming growth factor Beta 3 is required for excisional wound repair in vivo. *PLoS One.* 2012; 7(10): e48040. doi: [10.1371/journal.pone.0048040](https://doi.org/10.1371/journal.pone.0048040).
 28. Chong DLW, Trinder S, Labelle M, Rodriguez-Justo M, Hughes S, Holmes AM, *et al.* Platelet-derived transforming growth factor-beta1 promotes keratinocyte proliferation in cutaneous wound healing. *J Tissue Eng Regen Med.* 2020; 14(4): 645–9.
 29. Wu LW, Chen WL, Huang SM, Chan JY. Platelet-derived growth factor-AA is a substantial factor in the ability of adipose-derived stem cells and endothelial progenitor cells to enhance wound healing. *FASEB J.* 2019; 33(2): 2388–95.
 30. Gartner MH, Benson JD, Caldwell MD. Insulin-like growth factors I and II expression in the healing wound. *J Surg Res.* 1992; 52(4): 389–94.
 31. Geiger BC, Wang S, Padera RF, Grodzinsky AJ, Hammond PT. Cartilage-penetrating nanocarriers improve delivery and efficacy of growth factor treatment of osteoarthritis. *Sci Transl Med.* 2018; 10(469): eaat8800.
 32. Takeuchi M, Kamei N, Shinomiya R, Sunagawa T, Suzuki O, Kamoda H, *et al.* Human platelet-rich plasma promotes axon growth in brain-spinal cord coculture. *Neuroreport.* 2012; 23(12): 712–6.
 33. Sowa Y, Kishida T, Tomita K, Adachi T, Numajiri T, Mazda O. Involvement of PDGF-BB and IGF-1 in activation of human Schwann cells by platelet-rich plasma. *Plast Reconstr Surg.* 2019; 144(6): 1025e–36.
 34. Li Y, Zhang J, Yue J, Gou X, Wu X. Epidermal stem cells in skin wound healing. *Adv Wound Care (New Rochelle).* 2017; 6(9): 297–307.
 35. Mascré G, Dekoninck S, Drogat B, Youssef KK, Brohéé S, Sotiropoulou PA, *et al.* Distinct contribution of stem and progenitor cells to epidermal maintenance. *Nature.* 2012; 489(7415): 257–62.
 36. Tong L. *The experimental research of applying autologous platelet-rich gel to therapy deep II burn wound (in Chinese).* University of South China, 2011.
 37. Thompson KB, Krispinsky LT, Stark RJ. Late immune consequences of combat trauma: a review of trauma-related immune dysfunction and potential therapies. *Mil Med Res.* 2019; 6(1): 11–24.
 38. Hua Y, Bergers G. Tumors vs. chronic wounds: an immune Cell's perspective. *Front Immunol.* 2019; 10: 2178–89.
 39. Mariani E, Canella V, Cattini L, Kon E, Marcacci M, Matteo BD, *et al.* Leukocyte-rich platelet-rich plasma injections do not up-modulate intra-articular pro-inflammatory cytokines in the osteoarthritic knee. *PLoS One.* 2016; 11(6): e0156137.
 40. Potente M, Gerhardt H, Carmeliet P. Basic and therapeutic aspects of angiogenesis. *Cell.* 2011; 146(6): 873–87.
 41. Zachary I. VEGF signalling: integration and multi-tasking in endothelial cell biology. *Biochem Soc Trans.* 2003;31(Pt 6): 1171–7.
 42. Yu C, Xu ZX, Hao YH, Gao YB, Yao BW, Zhang J, *et al.* A novel microcurrent dressing for wound healing in a rat skin defect model. *Mil Med Res.* 2019; 6(1): 22–31.
 43. Weng T, Wu P, Zhang W, Zheng Y, Li Q, Jin R, *et al.* Regeneration of skin appendages and nerves: current status and further challenges. *J Transl Med.* 2020; 18(1): 53–70.
 44. Paththinige ND, Akarawita JKW, Jeganathan G. The clinical efficacy and safety of autologous activated platelet-rich plasma injection in Androgenetic alopecia. *Skin Appendage Disord.* 2020; 6(1): 19–24.
 45. Gentile P, Garcovich S. Autologous activated platelet-rich plasma (AA-PRP) and non activated (A-PRP) in hair growth: a retrospective, blinded, randomized evaluation in androgenetic alopecia. *Expert Opin Biol Ther.* 2020; 20(3): 327–37.
 46. Zhu M, Kong D, Tian R, Pang M, Mo M, Chen Y, *et al.* Platelet sonicates activate hair follicle stem cells and mediate enhanced hair follicle regeneration. *J Cell Mol Med.* 2020; 24(2): 1786–94.
 47. Xiao S, Wang J, Chen Q, Miao Y, Hu ZQ. The mechanism of activated platelet-rich plasma supernatant promotion of hair growth by cultured dermal papilla cells. *J Cosmet Dermatol.* 2019; 18(6): 1711–6.
 48. Zeng XL, Sun L, Zheng HQ, Wang GL, Du YH, Lv XF, *et al.* Smooth muscle-specific TMEM16A expression protects against angiotensin II-induced cerebrovascular remodeling via suppressing extracellular matrix deposition. *J Mol Cell Cardiol.* 2019; 134: 131–43.
 49. Yang L, Witten TM, Pidaparti RM. A biomechanical model of wound contraction and scar formation. *J Theor Biol.* 2013; 332: 228–48.
 50. Rosadi I, Karina K, Rosliana I, Sobariah S, Afini I, Widyastuti T, *et al.* In vitro study of cartilage tissue engineering using human adipose-derived stem cells induced by platelet-rich plasma and cultured on silk fibroin scaffold. *Stem Cell Res Ther.* 2019; 10(1): 369–84.
 51. Hinz B, McCulloch CA, Coelho NM. Mechanical regulation of myofibroblast phenoconversion and collagen contraction. *Exp Cell Res.* 2019; 379(1): 119–28.
 52. Ribatti D, Tamma R. Giulio Gabbiani and the discovery of myofibroblasts. *Inflamm Res.* 2019; 68(3): 241–5.
 53. Xiang Z, Zhou Q, Hu M, Sanders YY. MeCP2 epigenetically regulates alpha-smooth muscle actin in human lung fibroblasts. *J Cell Biochem.* 2020; 121(7): 3616–25.